

## INTEGRATED LIGHTWEIGHT, GLASS-FREE PV MODULE TECHNOLOGY FOR BOX BODIES OF COMMERCIAL TRUCKS

Christoph Kutter<sup>1</sup>, Felix Basler<sup>1</sup>, Luis Eduardo Alanis<sup>1</sup>, Jochen Markert<sup>1</sup>, Martin Heinrich<sup>1</sup>, Dirk Holger Neuhaus<sup>1</sup>

<sup>1</sup>Fraunhofer Institute for Solar Energy Systems ISE, Heidenhofstrasse 2, 79110 Freiburg, Germany

Corresponding author: Christoph Kutter | Phone: +49 (0)761 4588 2196 | e-mail: christoph.kutter@ise.fraunhofer.de

**ABSTRACT:** We propose a new integrated photovoltaic module technology and manufacturing process for the seamless integration into box body roofs of commercial trucks to unlock a 90.2 GW potential in the EU. Our approach is to laminate c-Si photovoltaic cells with an ETFE-top cover onto conventional GFRP-hard-foam sandwich elements, which can be directly installed with conventional box body profiles. We find that VIPV modules must be lead-free and report results of Hot-Spot, Wet-leakage test and insulation tests to prove the electrical safety of the new concept. We perform UV, DH and accelerated TC testing on minimodules and find a mean  $P_{MPP}$  drop of 3.6% for PERC, ribbon soldered half-cell modules after accelerated TC200 due to finger failure and partial ribbon disconnections. We conclude that conventional soldered ribbon based interconnection in combination with polymer based cover materials lead to unfavorable thermomechanical stresses in TC. We propose the usage of interconnection technologies that are less sensitive to thermomechanical stresses like Multiwire or shingling as we find that the mean drop in  $P_{MPP}$  of shingle modules to be 1%. PERC Solar cells encapsulated using the proposed module design remain stable after DH1000 and UV 60 kWh/m<sup>2</sup>. We equipped a *Mega electronics e-Worker* with a photovoltaic active box body featuring the first generation of proposed module technology and reported initial monitoring results after 10 months of outdoor operation.

**Keywords:** VIPV, Vehicle integrated photovoltaics, trucks, lightweight, glass-free, PV module, ETFE

### 1 INTRODUCTION

Vehicle-Integrated Photovoltaic (VIPV) in general is a promising solution to reduce primary energy consumption and carbon emissions in the mobility sector.[1] Measurement studies conducted by Fraunhofer ISE on moving 40t-trucks in central Europe and the greater New York area reveal that a DC-yield of 5,300 and 7,395 kWh/a per truck can be generated with 18 % efficiency module technology. [2] Assuming an electricity demand of 125 kW per 100 km e.g. of the announced Tesla Semi [3] and a yearly driving distance of 95,389 km (German average for a tractor unit [4]), at least 4.4% for the greater New York area and 6.2 % for central Europe of the yearly energy demand could be covered by the integrated PV system.

More than 39.7 Million light, medium and heavy duty vehicles (6,6 Million > 3.5 t) were operated in the EU in 2019 [5]. Based on 2018 German vehicle licensing data, heavy duty vehicles (> 3,5 t) hold an estimated average roof surface area of 21.5 m<sup>2</sup> [6]. This constitutes a technical VIPV potential (21 % efficiency, 95 % usable roof area) for commercial vehicles of more than 90.2 GW for the EU (Germany, 8 GW).

With a share of 26.3 %, trucks' and buses' contribution to road transport related EU green-house gas emissions in 2017 accounted for ~180 MtCO<sub>2</sub>e [7]. As a result, a yearly CO<sub>2</sub> saving potential of 11.5 MtCO<sub>2</sub>e can be estimated by the utilization of solar energy through VIPV on commercial vehicles in the EU. In order to unlock this potential we propose a lightweight, glass-free module technology. The presented module technology allows for a resource and cost efficient integration of PV into box bodies. The solar active body panels are compatible with conventional box body structures enabling an easy implementation of the innovative technology providing a path for PV-applications in commercial vehicles.

### 2 MODULE TECHNOLOGY

#### 2.1 New requirements for VIPV Modules

The safety and functionality related requirements towards automotive integrated photovoltaic modules arise from the established PV standards as well as standards from automotive frameworks. Selected standards and regulations are mentioned below.

VIPV Modules are photovoltaic modules and therefore need to meet the safety requirements according to IEC 61730.

DIRECTIVE 2011/65/EU on the restriction of the use of certain hazardous substances in electrical and electronic equipment defines an exception for "photovoltaic panels intended to be used [...] at a defined location". Road-mobile PV-panels therefore are not covered by that exception and conclusively need to be lead-free. [8]

Regulation ECE-R100, which addresses provisions concerning the approval of vehicles with regard to specific electric power train requirements, defines a 'high voltage level' (> 60 V<sub>DC</sub>) that requires additional safety measures e.g. insulation resistance monitoring and voltage drop rates after opening of connectors. [9]

In consequence when multiple modules are connected in series, with a system voltage that exceeds 60 V<sub>DC</sub>, additional safety measures need to be implemented to guarantee that the voltage drops below 60 V<sub>DC</sub> within 1 s after connectors are opened or cables or modules are damaged.

#### 2.2 Module Concept and Approach

The glass-free module technology is based on conventional hard-foam box body panels. [10] The box body panel used in this study is made up of two glass-fiber reinforced plates that encompass a hard-foam core. Due to the tensile strength of the glass fibers the structure is extremely rigid and torsion-resistant. Glass is not technically feasible as a top cover for VIPV modules, as area specific weight is too high and rupture safety in case

of an accident or torsion of the box body is not guaranteed. Hence we use weather resistant ETFE foil as a front cover as illustrated in Figure 1.

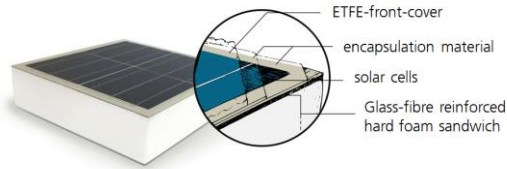


**Figure 1:** Schematic cross section of the box body module technology

Junction Boxes and Cables are embedded in the hard foam core of the sandwich element. The additional weight by integrating the PV-functionality to conventional sandwich elements is minimal with  $< 1.4 \text{ kg/m}^2$ .

### 2.3 Manufacturing process

The automated soldering interconnection of half cut Passive Emitter Rear Cells (PERC) was performed with a *Teamtechnik TT1800*. The shingling interconnection of 1/5 PERC shingled cells was done using a *Teamtechnik TT1600 ECA*. [11]

For lamination we used a *Bürkle E-LAPV Laminator* with a bottom heating plate (bottom) and an optional heating capable membrane (top). Due to the flexible elastic front cover foil a sunny side up lamination approach would be beneficial. However, the foam core of the body panel acts as a heat insulator. Therefore, the heat transfer from the heating plate through the sandwich element in a sunny-side-up lamination approach is very limited and the heat flow through the membrane is not sufficient to reach the required temperature for the encapsulant to crosslink. In order to manufacture these panels in a conventional PV-Laminator at Fraunhofer ISE's laboratory ModuleTec, we developed a sunny-side down lamination process where the module layup is done on a heat conductive carrier. The whole setup is moved into the laminator and processed at  $160^\circ\text{C}$  for 10 mins. The process is applicable in conventional industrial laminators.

### 2.4 Module format for box bodies in commercial vehicles

Within the European Union the width of commercial transportation vehicles is regulated. The directive EU 2015/719 and national road traffic regulations define maximum vehicle dimensions. For utility vehicles and therefore box bodies, the maximum width is 2.55 m. Cooling trucks built of insulation walls with a thickness  $> 45 \text{ mm}$  must not be wider than 2.60 m. [12]

Based on the standardized vehicle dimensions we suggest standardized module dimensions to be  $2.50 \times 1 \text{ m}^2$  as the structural integrity of the box body benefits from continuous roof-panels across the movement direction of the vehicle.

## 3 RELIABILITY TESTING

To prove the suitability and reliability of the proposed module technology, selected Module Safety and Module Quality Tests according to IEC 61730 and IEC 61215 were performed on laminates featuring the setup illustrated below (Figure 2).

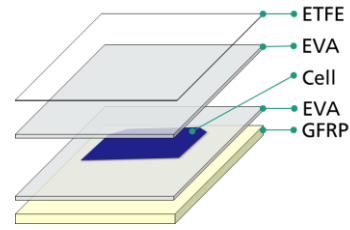


**Figure 2:** Schematic material stack of the tested laminates (ETFE – Ethylene tetrafluoroethylene, EVA – Ethylene-vinyl acetate, GFRP – glass fiber reinforced plastic)

Insulation Test (MQT 03), and Wet leakage current test (MQT 15) were performed before and after a Hot-spot endurance test (MQT 09) on a 60-full-cell-laminate, (see Figure 3). The maximum cell temperature reached during the Hot-Spot endurance test was  $146^\circ\text{C}$  when cell A8 was shaded 25 %.

No visual defects were found and the module passed Wet leakage and insulation tests afterwards.

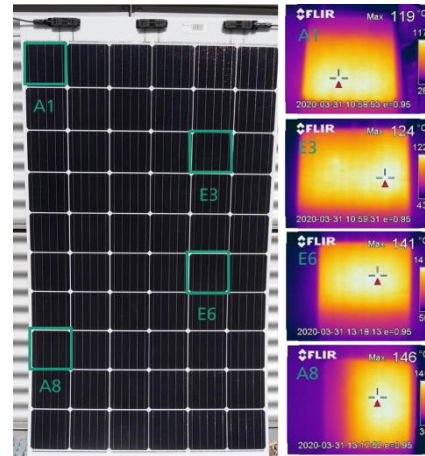


**Figure 3:** Photo of module after Hot-Spot endurance test, with marked shaded cells. Infrared images of the respective shaded cell and highest measured temperatures during Hot-Spot endurance testing

Minimodules with PERC half cells and PERC shingle strings were built and exposed to environmental testing. The used GFRP material for the minimodules featured no gelcoat layer.

Three half-cell modules have undergone UV-Testing with cumulative dose of 15, 30 and  $60 \text{ kWh/m}^2$ . Four half-cell modules have been exposed to 1,500 h Damp heat testing in 500 h steps.

The accelerated thermal cycling (aTC) procedure proposed by Schiller et al. with higher heating/cooling rates ( $8 \text{ K/min}$ ) and a 25 min dwell time was applied on four half-cell modules and four shingle modules [13].

After each testing step the modules have been I-V and EL characterized at Fraunhofer ISE's ModuleTEC. The IV-measurements have been analytically temperature-corrected to  $25^\circ\text{C}$ . The used PERC cells were not stabilized for Light induced degradation (LID) [14] and light and elevated temperature induced degradation (LETID) [15].

After aTC200 we found the half-cell laminates mechanically intact and no delamination of the encapsulation was observed. The GFRP exhibits minor

yellowing. Figure 4 shows a photographic comparison of a module before and after aTC200.

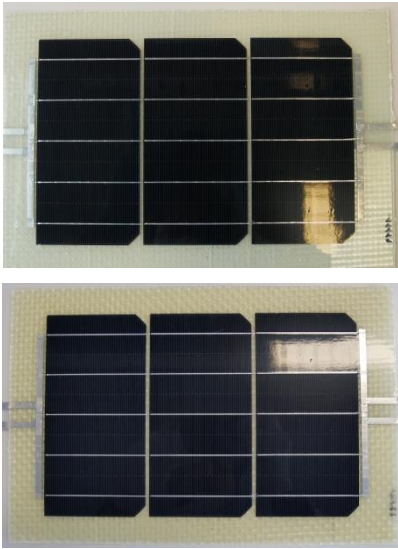


**Figure 4:** Photographs of a half-cell module initially (top) and after aTC200 (bottom)

Electrically, we observe that the emitted light intensity of the half cells in electroluminescence (EL) images becomes more inhomogeneous (Fig. 5), due to two effects: finger failure and partial disconnected cell-interconnect-ribbons. [16, 17]

Finger failure typically indicates a high strain at the solder joint. It is commonly known that this kind of failure appears after thermomechanical stresses and lead to power losses in the TC test.

All cells tend to darken from the pseudo-square-edge, where the ribbon is led from the front side of the cell to the rear of the neighboring cell (Figure 5).

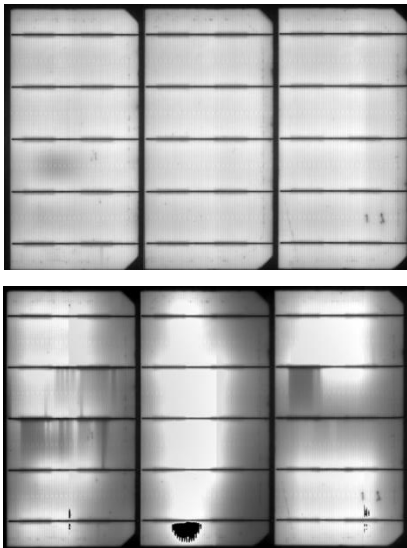


**Figure 5:** EL-images of 3-half-cell module before (top) and after aTC200 (bottom)

From Finite Element Modelling (FEM) of modules with polymeric top covers we know that ribbon tend to compress at -40 °C inducing vertical shear stress on the contact-metallization-interface (Figure 6).

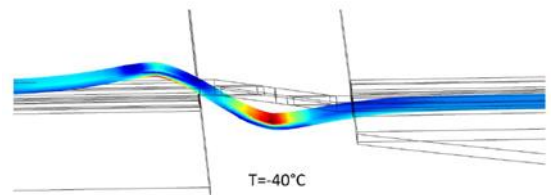


**Figure 6:** FEM distortion result for a soldered ribbon at -40 °C with a polymer-based top cover (double scaled)

Our assumption is that the tested polymeric top cover in comparison to glass does not have enough rigidity to counterweight the ribbon compression-induced forces. Additionally, finger failure and ribbon disconnection effects are intensified due to the higher thermal expansion of the ETFE top cover, which is  $9.4 \times 10^{-5} \text{ K}^{-1}$  [18] vs.  $9 \times 10^{-6} \text{ K}^{-1}$  of soda-lime-glass [19]. Therefore the soldered joint between cell metallization and ribbon or cell is subject to fatigue failure at the cell edges in aTC.

This is backed by the analysis of the reference module. We find the finger failure effect to be less strong in the reference module with glass-backsheet configuration. The ribbon disconnect effect is not present in the reference module after aTC200 (Figure 7).

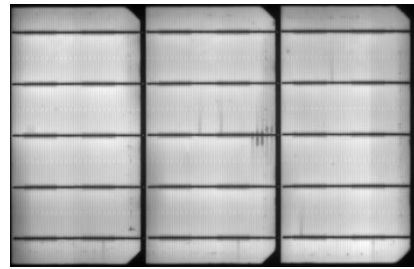


**Figure 7:** EL-image of the glass-backsheet reference after aTC200

The box plot in Figure 8 illustrates the relative change of the electrical parameters of all four ETFE half-cell modules and the glass-backsheet reference for 50, 100 and 200 aTC cycles. We see a 0.2% increase of the  $I_{sc}$  and only a 0.4% decrease in  $V_{OC}$  after 200 cycles. Average fill factor (FF) of the ETFE-modules degrades strongly by 3.6 % after 200 cycles, resulting in a 3.7 % average reduction of module power  $P_{MPP}$  compared to 2.5 % for the reference module.

The high drop in FF is typical when an increase of series resistance happens, which is the case for the two observed failure modes (finger failure and partial disconnected interconnection ribbons).

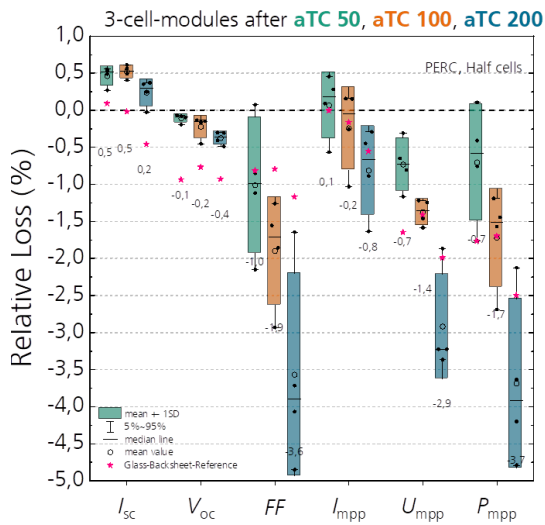


**Figure 8:** Relative losses after aTC – aging of half-cell-modules

The presented results indicate that for the proposed ETFE-GFRP module interconnection technologies that induce less mechanical stress, e.g. shingled or multi-wire connection through smaller wire diameters, might be beneficial for better TC performance. Multiwire modules have been observed to show better TC performance in other studies. [13]

After aTC200 aging of the shingle modules we find the module configuration to remain intact, with no delamination observed (Figure 10). The front ETFE foil, as well as the rear GFRP cover, shows no damage. Again, the GFRP shows a minor yellowing.

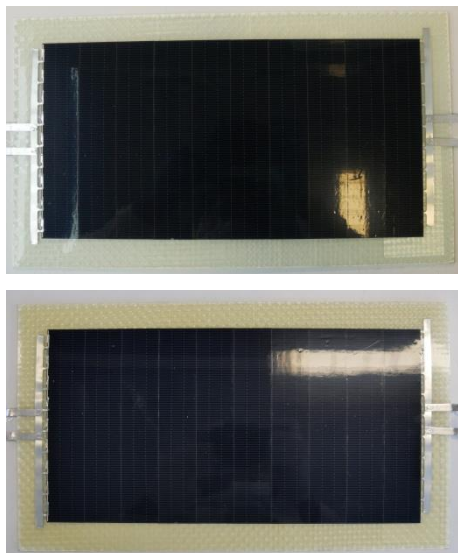


**Figure 9:** shingle-cell module (ID 11173) initially (top) and after aTC200 (middle)

After aTC200 aging of the shingle modules we observe a much more homogenous EL image of the modules as compared to the half-cell samples (Figure 11). There are no finger defects visible, which confirms our presumption that the ribbons are likely to cause the finger defects within conventional soldered ribbon technology.

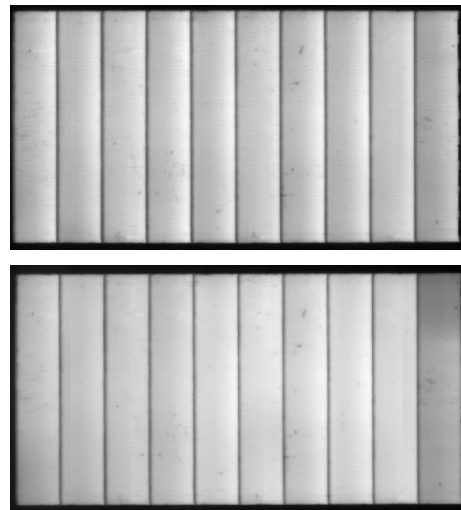


**Figure 10:** EL-images of 10-shingle-cell module initially (top) and after aTC200 (bottom)

The promising EL images are backed by electrical measurements shown in Figure 11. Relative mean power drop in  $P_{MPP}$  is only 1%. These findings are in good accordance with aTC results of shingle interconnection technologies reported by Schiller et al. [13]

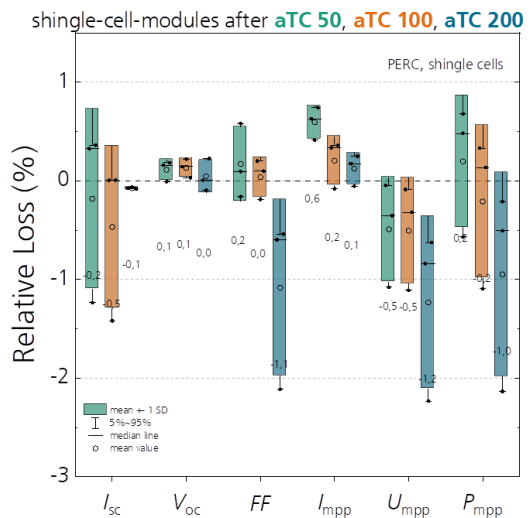


**Figure 11:** relative losses after aTC – aging of shingle modules

To evaluate the impact of hot humid climates on module reliability we exposed four half-cell-modules and one glass-backsheet reference to damp heat (DH) testing at 85 °C and 85 % relative humidity. DH is known to challenge the adhesion of the module compounds. DH exposes lack of edge sealing and insufficient tightness due to visible corrosion of cells and connectors.

After 1,500 h of DH exposure we observe visible deterioration of the module compounds due to embrittlement of the GFRP (Figure 12). The cell and cross connectors show partial corrosion and small areas of delamination on top of the corroded cell connectors can be observed.

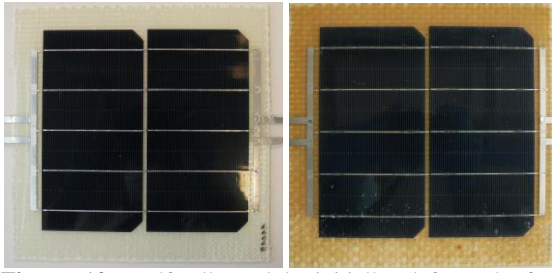


**Figure 12:** Half-cell module initially (left) and after DH1,500 (right)

The EL images in Figure 13 after DH1,500 show signs of corrosion at cell edges as well as the cell connector edges.

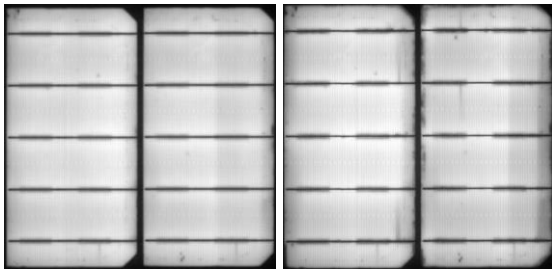


**Figure 13:** EL-image of a half-cell module initially (left) and after DH1500 (right)

We find similar deterioration effects after DH1500 in the glass-backsheet-reference (Figure 14).

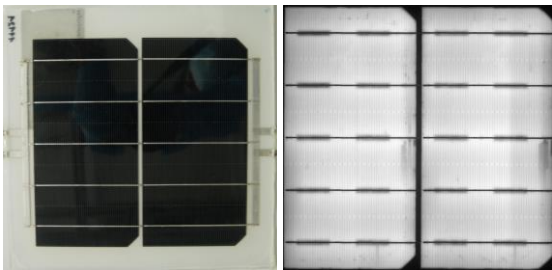


**Figure 14:** Photograph (left) and EL image (right) of glass-backsheet reference after DH1500

Analyzing the mean relative losses of the electrical module parameters in Figure 15, we observe a mean  $P_{MPP}$  change of -5 % after DH1500 (-2.5 % after DH1000), which is -2.5 % more than the glass-backsheet reference module.

We expect that the sandwich elements framed and sealed within the box body (Figure 18) will see much less exposure to humidity, therefore embrittlement of the GFRP should be less relevant. Furthermore, applying a gelcoat to the exposed surfaces of the GFRP is a well-known approach to improve weather stability of GFRP [21].

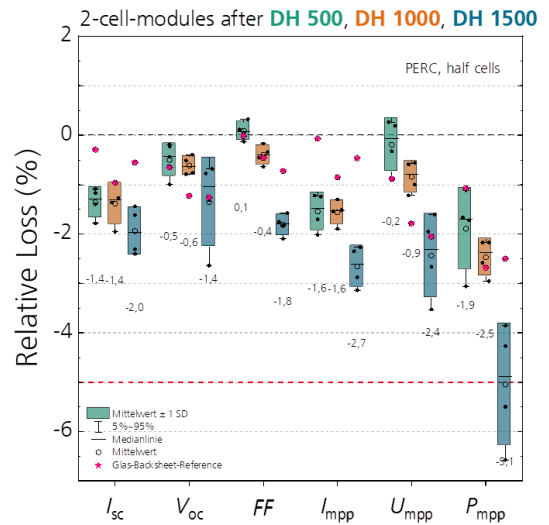


**Figure 15:** relative losses after DH – aging of half-cell-modules

To determine the UV weathering resistance of the glass-free module concepts, three half-cell modules were conditioned with 15, 30 and 60 kWh/m<sup>2</sup> of UV light from the front side according to MQT 10 of IEC61215.

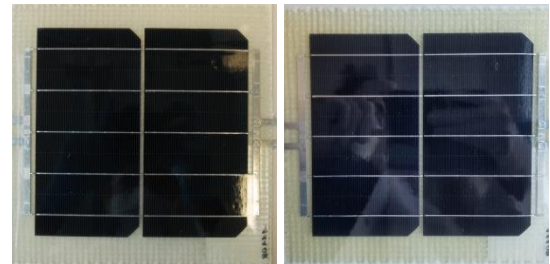


**Figure 16:** Half-cell module initially (left) and after UV 60 kWh/m<sup>2</sup> (right)

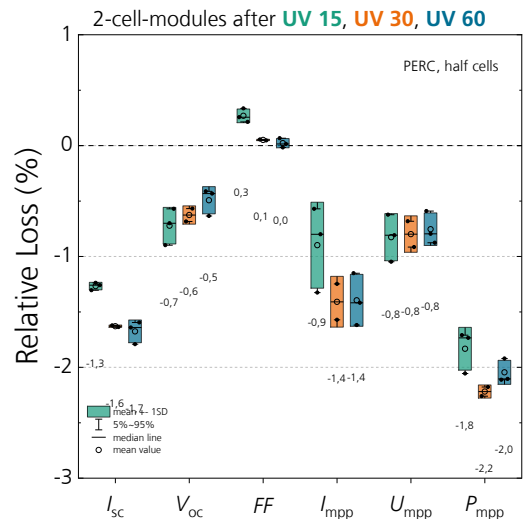


**Figure 17:** Relative losses after UV-aging

We found no visible deterioration of the module compounds after conditioning with 60 kWh/m<sup>2</sup> (Figure 16). Although by visual inspection and EL imaging no damages could be identified, average module power output drops by 2 % while FF slightly increases (Figure

17). This is only possible since  $I_{sc}$  drops quite significantly by 1.7 %. A possible reason could be degradation within the EVA encapsulant resulting in increased absorption or reflection within the EVA layer. Further validation experiments to identify the degradation mechanisms are planned.

#### 4 OUTDOOR EXPOSURE - DEMOTRUCK

In fall 2019 a *Mega electronics e-Worker* was equipped with a vehicle integrated PV box body by *TFS Fahrzeugbau GmbH* in Umkirch, Germany. The modules are embedded and installed via conventional aluminum box body frames and additionally sealed with silicon sealants. The sides of the box body can be orientated to the sun (Figure 18).

The first module generation, featuring shingled solar cells and initial interconnection technology based on Electrically Conductive Adhesives (ECA) were developed at Fraunhofer ISE's ModuleTEC. [11] The 6 modules, installed on the sides and roof (Figure 18), achieve a peak power of 990 W and are connected to the drive train battery via a DC-DC-Converter. The vehicle is in daily outdoor operation at Fraunhofer ISE's campus in Freiburg, Germany.

The truck is monthly monitored by visual inspection and every half year the modules are tested using EL imaging to detect any ageing effects. During the 10 months of outdoor exposure (September 19 – July 20), the modules have experienced different environmental loads such as high irradiation at elevated ambient temperatures, snow, rain, heat and soiling (Figure 19).



**Figure 18:** Fraunhofer ISEs *Mega electronics e-worker* with PV-box body

It was found that the module setup withstands the observed conditions robustly. After 10 months of operation no delamination is observed, the cover foils remain intact.

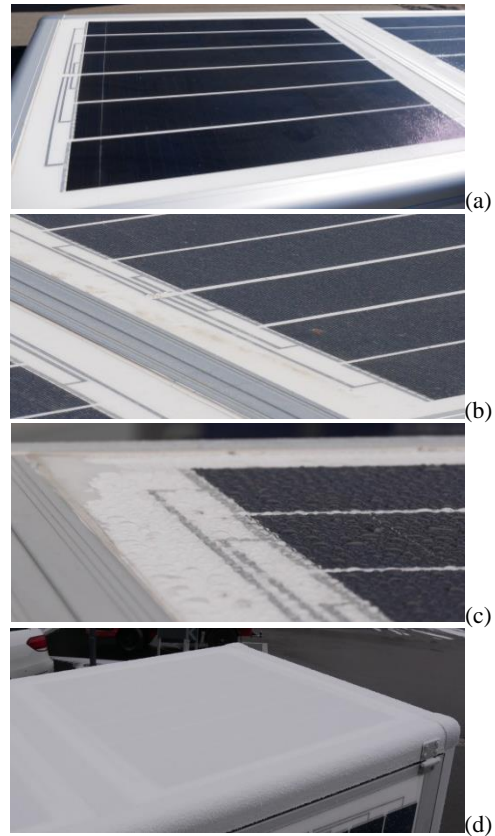


**Figure 19:** Environmental loads: High irradiation at ambient temperatures of  $>35^{\circ}\text{C}$  during summer 2020 (a); soiling due to pollen during spring 2020 (b); rain (c) and snow cover during winter 2020 (d)

Further minor damages have been found where an external mechanical force was certainly at play (Figure 20).

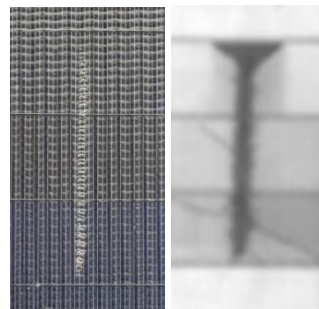


**Figure 20:** Scratch on the surface of the ETFE foil (left) damaged cells in the EL image (right)

With the EL imaging we find that the emitted radiation levels of the shingled solar cells become more inhomogeneous in the EL image after environmental exposure (Figure 21). This might indicate a deterioration process of the cells or the ECA joint. The shingled solar cells remain mechanically intact. We would like to highlight that unlike the minimodules that were put into the ageing experiment featured optimized cells and enhanced ECAs, the modules in this section have been manufactured with first generation cells and non-optimized processes. Therefore, new exposure experiments on vehicles with the enhanced bill of materials are planned.

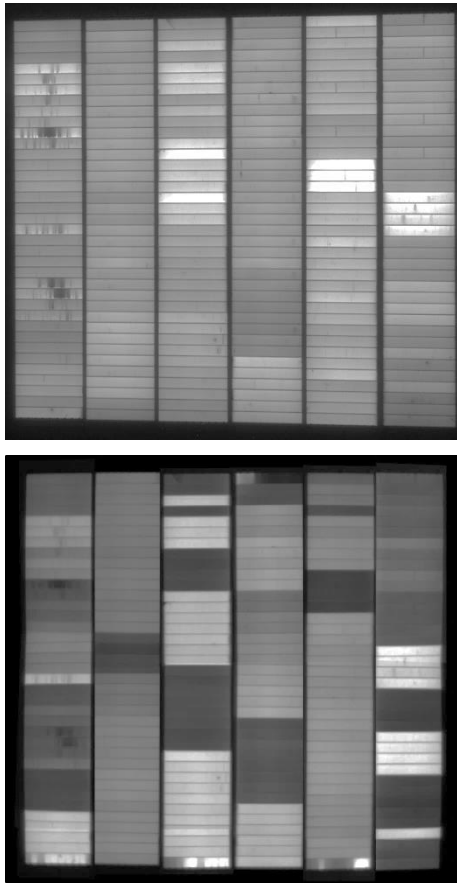


**Figure 21:** Module 5, EL image taken with *Great Eyes* EL system in a dark chamber after lamination in Sep. 19 (top), EL image in July 2020 taken with *Xenics InGaAs* camera outdoors (bottom)

## 5 CONCLUSION

We propose a module technology that integrates c-Si cells directly into box bodies of commercial vehicles. Our approach is to laminate the c-Si cells together with an ETFE top cover foil onto conventional GFRP-hard-foam sandwiches in a sunny-side-down lamination process. We find maximum hot-spot temperatures in a 60-cell laminate to be uncritical. Afterwards the sample module passes wet-leakage and insulation tests. After UV60 cells remain intact and show no sign of deterioration other than slight GFRP yellowing. After DH 1,500 the embrittlement of GFRP (no gelcoat) allows humidity to enter and corrosion of connectors and cell edges is observed. Exposure to 200 aTC-Cycles reveal a sensitivity to thermomechanical stresses of soldered ribbon technology ( $-3.6\% \Delta P_{MPP}$ ) in our polymer based module technology. Shingled mini modules show a better aTC performance ( $-1\% \Delta P_{MPP}$ ). We propose to further investigate the combination of the GFRP-ETFE module concept with interconnection technologies that are known to be less sensitive to thermomechanical stresses e.g. shingling and Multiwire.

The monitoring results of a *Mega electronics e-Worker* that was equipped with PV panels and operated for 10 months in Freiburg, Germany, show promising real world weather resistance of the proposed module technology.

## 6 OUTLOOK

Within the project Lade-PV (FKZ 03EE1002A) we will further develop and test (e.g. Hail-Test) the introduced module technology as well as develop the system technology to feed the photovoltaic energy directly into the high voltage drive train of the vehicle. With the 2<sup>nd</sup> module generation we will equip a box body of a *Framo E-165* truck and test for weathering and further environmental exposure typically observed in this setup.

## 7 ACKNOWLEDGEMENT

We thank Dominic Röder for FEM simulation of the ribbon kink, Franziska Katzmaier and Stephan Hoffmann for EL-Characterization and Leen Abdin for IV-characterization of the presented modules.

We would like to thank the German Ministry of Economic Affairs and Energy for their funding under the contract number (FKZ 03EE1002A “Lade-PV”).

## 8 REFERENCES

- [1] M. Heinrich, C. Kutter, F. Basler, M. Mittag, E. Alanis, D. Eberlein, A. Schmid, C. Reise, T. Kroyer, H. Neuhaus, H. Wirth, “Potential and Challenges of Vehicle Integrated Photovoltaics for Passenger Cars,” in *37th EU PVSEC 2020*.
- [2] U. Eitner *et al.*, “Solar Potential on Commercial Trucks: Results of an Irradiance Measurement Campaign on 6 Trucks in Europe and USA,” in *Proceedings of the 33rd European Photovoltaic Solar Energy Conference and Exhibition (EU PVSEC)*, Amsterdam, 2017, pp. 2147–2150.
- [3] I. Tesla, *Tesla Semi: Product website*. [Online]. Available: <https://www.tesla.com/semi> (accessed: 18.08.20).
- [4] Kraftfahrtbundesamt (KBA), “Verkehr in Kilometern - Inländerfahrleistung (VK),” 2019. [Online]. Available: [https://www.kba.de/DE/Statistik/Kraftverkehr/VerkehrKilometer/verkehr\\_in\\_kilometern\\_node.html](https://www.kba.de/DE/Statistik/Kraftverkehr/VerkehrKilometer/verkehr_in_kilometern_node.html)
- [5] European Automobile Manufacturers Association, “Vehicles in use - Europe 2019,” 2017. Accessed: 11.12.19. [Online]. Available: [https://www.acea.be/uploads/publications/ACEA\\_Report\\_Vehicles\\_in\\_use-Europe\\_2019.pdf](https://www.acea.be/uploads/publications/ACEA_Report_Vehicles_in_use-Europe_2019.pdf)
- [6] Kraftfahrt-Bundesamt, *Fahrzeugzulassungen im Dezember 2018 - Jahresbilanz: Pressemitteilung Nr. 01/2019*, 2019. Accessed: Dec. 10 2019. [Online]. Available: [https://www.kba.de/SharedDocs/Pressemitteilungen/DE/2019/pm\\_01\\_2019\\_fahrzeugzulassungen\\_12\\_2018\\_pdf.pdf?\\_\\_blob=publicationFile&v=6](https://www.kba.de/SharedDocs/Pressemitteilungen/DE/2019/pm_01_2019_fahrzeugzulassungen_12_2018_pdf.pdf?__blob=publicationFile&v=6)
- [7] sni, *The European environment - state and outlook 2020: Knowledge and transition to a sustainable Europe*, 2019. [Online]. Available: <https://www.eea.europa.eu/publications/soer-2020>
- [8] *DIRECTIVE 2011/65/EU OF THE EUROPEAN PARLIAMENT AND OF THE COUNCIL of 8 June 2011 on the restriction of the use of certain hazardous substances in electrical and electronic equipment: DIRECTIVE 2011/65/EU*, 2011. Accessed: 12.08.20. [Online]. Available: <https://eur-lex.europa.eu/legal-content/EN/TXT/?uri=CELEX:02011L0065-20200501>
- [9] *Regulation No 100 of the Economic Commission for Europe of the United Nations (UNECE)* —

- Uniform provisions concerning the approval of vehicles with regard to specific requirements for the electric power train [2015/505]: UNECE R100*, 2015. Accessed: 12.08.20. [Online]. Available: <https://op.europa.eu/en/publication-detail/-/publication/fd8e6b47-d767-11e4-9de8-01aa75ed71a1/language-de>
- [10] M. M. Matthieu Ebert, "Photovoltaic Module and Container Equipped Therewith," US20190084428A1, DE.
- [11] P. Baliozian *et al.*, *PERC-based shingled solar cells and modules at Fraunhofer ISE*. [Online]. Available: <https://www.pv-tech.org/photovoltaics-international/photovoltaics-international-volume-43> (accessed: Dec. 2 2019).
- [12] *DIRECTIVE (EU) 2015/719 OF THE EUROPEAN PARLIAMENT AND OF THE COUNCIL amending Council Directive 96/53/EC laying down for certain road vehicles circulating within the Community the maximum authorised dimensions in national and international traffic and the maximum authorised weights in international traffic: DIRECTIVE (EU) 2015/719*, 2015. Accessed: Aug. 12 2020. [Online]. Available: <https://op.europa.eu/en/publication-detail/-/publication/22b313fc-f3bc-11e4-a3bf-01aa75ed71a1/language-en/format-PDF/source-search>
- [13] C. H. Schiller, L. C. Rendler, D. Eberlein, G. Mülhöfer, A. Kraft, and D. H. Neuhaus, "Accelerated TC Test in Comparison with Standard TC Test for PV Modules with Ribbon, Wire and Shingle Interconnection," in *Proceedings of the 36th European Photovoltaic Solar Energy Conference and Exhibition (EU PVSEC); Marseille, France*, 2019, pp. 995–999.
- [14] A. Herguth, G. Schubert, M. Kaes, and G. Hahn, "A New Approach to Prevent the Negative Impact of the Metastable Defect in Boron Doped CZ Silicon Solar Cells," pp. 940–943, doi: 10.1109/WCPEC.2006.279611.
- [15] E. Fokuhl, T. Naeem, A. Schmid, P. Gebhardt, T. Geipel, and D. Philipp, "LeTID: A comparison of test methods on module level," in *Proceedings of the 36th European Photovoltaic Solar Energy Conference and Exhibition*, Marseille, France, 2019.
- [16] J. Wendt, M. Traeger, M. Mette, A. Pfennig, and B. Jaeckel, "The link between mechanical stress induced by soldering and micro damages in silicon solar cells," in *Proceedings of the 24th European Photovoltaic Solar Energy Conference and Exhibition*, Hamburg, Germany, 2009, pp. 3420–3423.
- [17] M. Köntges, S. Kurtz, C. Packard, U. Jahn, K. A. Berger, and K. Kato, *Performance and reliability of photovoltaic systems: Subtask 3.2: Review of failures of photovoltaic modules : IEA PVPS task 13 : external final report IEA-PVPS*. Sankt Ursen: International Energy Agency Photovoltaic Power Systems Programme, 2014. [Online]. Available: <https://edocs.tib.eu/files/e01fb16/856979287.pdf>
- [18] AGC Chemicals, Fluoropolymers Business Group, "AGC Floun ETFE Film brochure: Fluon® ETFE Film ENG/5-2014," 2014. Accessed: 12.08.20. [Online]. Available: <https://www.agcce.com/brochurespdfs/sales/ETFEfilmEnglish.pdf>
- [19] S. Lohmeyer, *Werkstoff Glas: Sachgerechte Auswahl, optimaler Einsatz, Gestaltung und Pflege*. Renningen-Malmsheim: Expert-Verl., 2001.
- [20] *Terrestrial photovoltaic (PV) modules – Design qualification and type approval – Part 2: Test procedures*, IEC 61215-2:2016, 2016.
- [21] S. Paul, Ed., *Surface coatings: Science & technology*, 2nd ed. Chichester: Wiley, 1996.